URSI GASS 2023, Sapporo, Japan, 19 – 26 August 2023

On the use of SuperDARN Ground Backscatter Measurements for Ionospheric Propagation Model Validation

Joshua Ruck*(1), David Themens(1,2)
(1) Space Environment and Radio Engineering (SERENE) Group, University of Birmingham, Birmingham, UK;
e-mail: jxr879@student.bham.ac.uk
(2) Department of Physics, University of New Brunswick, Fredericton, NB, Canada

Abstract

High-frequency (HF), radars can regularly see beyond the horizon, with this non-line-of-sight (LOS) propagation achieved through the use of the ionosphere as a reflector. The Super Dual Auroral Radar Network (SuperDARN) is a global network of HF coherent scatter radars operating in the range of 8-20 MHz and provides a vast data set of oblique HF soundings. Ground backscatter (GB) measurements present within this data have found increasing utility over time, showing use for interferometer calibration and real time determination of ionospheric parameters including fof2. We present a method for utilizing this vast data set to assess propagation models using two-dimensional numerical ray tracing to simulate the time evolution of ground backscatter echoes. Model and SuperDARN Leading Edge (LE) slant range is extracted and compared, showing errors of between 50- and 300-km for the daytime IRI. Here we will comprehensively demonstrate and assess the utility of this data for validation.

1 Introduction

By operating in the HF band (3-30 MHz), radars can regularly see beyond the horizon, with ground ranges in some cases exceeding 3,500 km [1]. This beyond line-of-sight (BLOS) propagation is achieved through the use of the ionosphere as a reflector, as within the HF band, this region of the upper atmosphere exhibits reflective properties and has a profound impact on the path of radio waves. Over-the-horizon radar (OTHR) systems exploit this phenomenon and are unique in their ability to detect targets at extreme ranges, offering cost-effective large area surveillance. The strategic advantage offered by OTHR is not understated, with many nations are pursuing development of such systems. A critical aspect of OTHR development is that of the coordinate registration (CR) system, which performs a transformation from radar to ground coordinates to provide geographical positioning of targets. This process requires highly accurate propagation models if one is to hope for reasonable positioning errors, and so it is paramount that the combination of ionospheric models and raytracing employed in the CR process is validated to ensure a representative reconstruction of the measured signal paths.

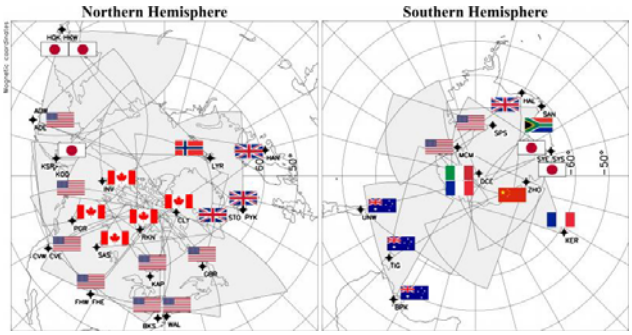

Figure 1. Map showing the geographical FOV coverage of the SuperDARN network of radars in the Northern (left) and Southern (right) hemispheres.

The Super Dual Auroral Radar Network (SuperDARN) is a global network of HF coherent scatter radars operating in the range of 8-20 MHz [2]. A total of 39 SuperDARN radars are distributed across both hemispheres at latitudes poleward from 30˚ either side of the equator as shown in Figure 1, with this expansive deployment providing an unparalleled coverage of ionospheric plasma dynamics at mid- to high-latitudes. The large field of view (FOV) of the radars, often between 51.84° and 77.76°, combined with BLOS propagation permits even single SuperDARN radars to cover vast geographical areas. Whilst signals backscattered by field aligned ionospheric irregularities are of primary interest to much of the community due to the information they provide on bulk plasma drifts, a significant proportion of the data provided by SuperDARN soundings is of ground backscatter (GB) origin. An important feature of these GB echoes is that they can be distinguished from ionospheric scatter due to their near zero doppler shift and other features characteristically different from ionospheric scatter, and so provide a useful secondary measurement within SuperDARN soundings. Measurements using SuperDARN have been conducted since the first radar was installed in 1983 at Goose Bay in Canada [3] and are regularly performed in real time at many of the radar sites, thus offering an expansive dataset of ground backscatter data. These GB measurements have found increasing utility over time, showing use for interferometer calibration [4] and real time determination of ionospheric parameters including fof2 [5] and maximum useable frequency (MUF) [6]. Climatological studies using GB data have also been performed by [7] and [8] to determine occurrence rates, with [7] additionally assessing the impact of the underlying ground scattering surface.

Although assessment of the IRI-2012 was conducted by Oinats et al [7], the use of GB data has not yet been explicitly employed for validation purposes to assess ionospheric models at timescales that capture diurnal to hourly variabilities and here, we describe a method for utilizing this vast data set to assess propagation models beyond the scope of climatology. Two-dimensional numerical ray tracing (NRT) is employed with the IRI2016 ionospheric model to simulate the time evolution of ground backscatter echoes, with skip distance extracted and compared for experimental and model data. In this paper, we will comprehensively demonstrate and assess the utility of this data for validation at hourly resolutions, which is important within the context of real time ionospheric models (RTIMs) to support OTHR CR and frequency management systems (FMS).

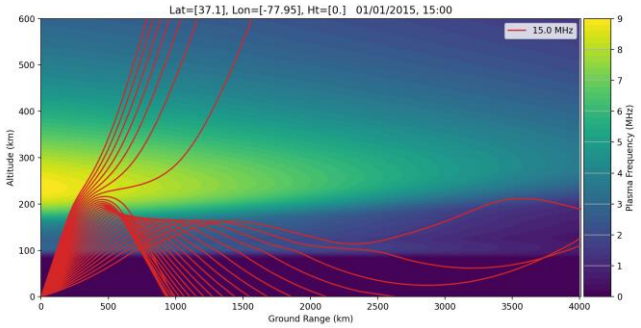

Figure 2. 2D raytrace from the Blackstone SuperDARN radar beam 4 at 15 MHz for elevations in the range 5°-40°.

2 Methodology

NRT is a technique widely employed to study HF propagation through the ionosphere and is well suited for simulating SuperDARN backscatter. NRT has been previously used by Perry et al [10] in the context of SuperDARN to validate the Saskatoon radar's gain pattern. This study makes use of the HFRM (high-frequency raytracing model) 2D NRT toolbox developed by the University of Birmingham's SERENE group and is used to model the expected signal paths for the Blackstone radar beam 4 with the IRI-2016 ionospheric model. The variation in GB for this beam during the time period 27th to 30th January 2016 is considered in this study, and it should be noted that this radar employs the newer twin terminated folded dipole (TTFD) antenna over the older log periodic (LPDA) design. An example 2D raytrace for this beam is presented in Figure 2. HFRM has previously been employed by SERENE to model a multi-static OTHR and uses an improved version of Coleman's NRT raytracer which is based on the Haselgrove set of equations [9]. In this study, a total of 250 rays are propagated at elevations between 5° and 40° at each time step within the SuperDARN data, with frequency set to match that of SuperDARN. Elevation is restricted to this range due to SuperDARN elevation measurements being unreliable at very high and low angles due to aliasing caused by the interferometer configuration. Ray landing points are then extracted and binned by group range into the same range bins as for the SuperDARN data. As the IRI has only an hourly resolution, generation of ionospheric grids at the minutely resolution of the SuperDARN data is not warranted and would provide an unnecessary computational expense. To overcome this issue, the IRI is only generated once every 15 minutes and interpolated between and whilst this is in excess of the model resolution, a finer generation time step is included to permit future work with assimilative models that operate with greater temporal resolutions.

To calculate the backscattered power for a given ray, an alternate form of the radar equation must be used and is given by the following

$$P_r = \frac{P_t G_t G_r}{L_{out} L_{in}} \frac{4\pi A_{eff} \sigma_0}{\lambda^2} \quad (1)$$

Where L corresponds to the combined propagation loss, A_{eff} the effective scattering area, σ_0 the backscatter coefficient, λ the wavelength and P and G are the power and gains at the transmit and receive sites, respectively. In this study a fixed backscatter coefficient of -26 dB is used which is a widely accepted reference value for backscatter from land; due to the beam selected from the Blackstone radar's FOV, backscatter from bodies of water is expected to contribute only minimally, thus warranting a single value. The effective area can be considered as the imposed area of a flux tube at the ground, and can be determined by the following equation:

$$A_{eff} = R_e sin\left(\frac{D}{R_e}\right) \frac{dD}{dP} \Delta P \Delta\Phi \quad (2)$$

Where D is the ground range, P the group range, ΔP the group range cell depth and $\Delta\Phi$ the azimuthal beamwidth. Calculation of the $\frac{dD}{dP}$ term is performed for pairs of rays in a fan. Azimuthal beamwidth is calculated using the empirical Equation 3, where the addition of the 1.12 constant was included to correct the relationship to the available data for the TTFD array provided in Sterne et al [10] at 10- and 14-MHz, showing an error of -1.18° at 10 MHz and matching exactly at 14 MHz.

$$\Delta\Phi = 50 \frac{\lambda}{L_{array}} + 1.12 \quad (3)$$

Unfortunately, array gain pattern data is not commonly available for the TTFD type antennas due to the novelty of their design, and so in this study we make use of the LPDA array gain data from Perry et al [8]. The primary difference between the TTFD and LPDA arrays besides the exact gain pattern is a slightly reduced maximum gain, and an increased beamwidth and front to back ratio. The overall impact of the different gain patterns is expected to be minimal within the elevation range of interest in comparison to propagation losses; however, future work will be conducted to obtain TTFD gain patterns to limit this source of difference.

3 Data Processing

Prior to comparison, the two data sets must be properly filtered and normalized to remove unwanted echoes and

match the power distribution. First, SuperDARN data is filtered to remove elevations outside of 5˚-40˚ to limit potential contamination by poor elevation data at high and low angles due to aliasing in the interferometry. As the principle interest of this study is 1-hop F-mode echoes, returns from the E-region and non 1-hops can be removed. A virtual height filter is applied to both data sets to remove these less desirable echoes and is calculated in the same manner as in Bland et al [6] using the following equation

$$h_v = \sqrt{r^2 + R_e^2 + 2rR_e sin\Delta} - R_e \qquad (4)$$

Echoes corresponding to a virtual height below 150 km are removed, as these are likely to contain E-mode, ½-hop, and meteor backscatter. Additionally, echoes with virtual heights above 600 km are also negated as these are expected to correspond to backscatter exceeding a single hop. Whilst the majority of meteor scatter is removed during this process, some remains, and this can easily be handled by removing echoes at slant ranges within 500 km.

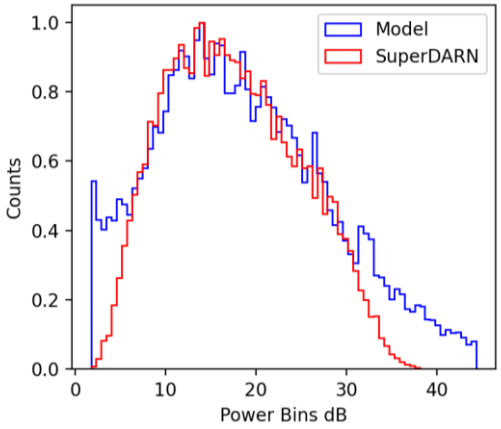

Figure 3. Histograms for SuperDARN and model power profiles after filtering and normalization of the model.

Issues arise when comparing the modelled and experimental power data, as the SuperDARN power values are in terms of the signal-to-noise ratio from a lambda fit of the ACF and so are difficult to replicate due to the exact receiver architecture and signal processing pipeline being unknown. To overcome this, the power profile of the modelled data is normalized in relation to the power distribution peaks found by binning power into 75 bins. Simulation data contains rays that would exist below the receiver threshold of the radar, thus being undetectable and requiring removal prior to our comparison. To this end, simulation data with power values below the minimum power of the SuperDARN power distribution are removed. Figure 3 shows the histograms for the two data sets after processing of the model profile, with this corresponding to a power offset of 72.34 dB being applied.

4 Results

To examine the capacity of the simulation to model the SuperDARN GB, the time evolution of backscatter echoes is plotted in Figures 6, demonstrating the variation in elevation angle. It should be noted that the local time is approximately 6 hours behind UTC. The LE of the GB is extracted by simply taking the minimum slant range at each time step and is overlaid on both figures in black. It is clear upon immediate inspection that significant differences in elevation angle occur between the two data sets, with the SuperDARN elevation data appearing to exceed that of simulation by approximately 5°-10°. A similar difference was observed by Oinats et al [9] and was attributed to underestimates in the IRI's representation of the electron density peaks. It is possible that this may also be attributed to calibration errors present within the Blackstone Interferometer setup. Small-scale variations observed in the SuperDARN GB at timescales of below 1-hour resolutions are not captured within the simulation as the IRI offers only a smoothed representation of the monthly median ionosphere at a limited temporal resolution.

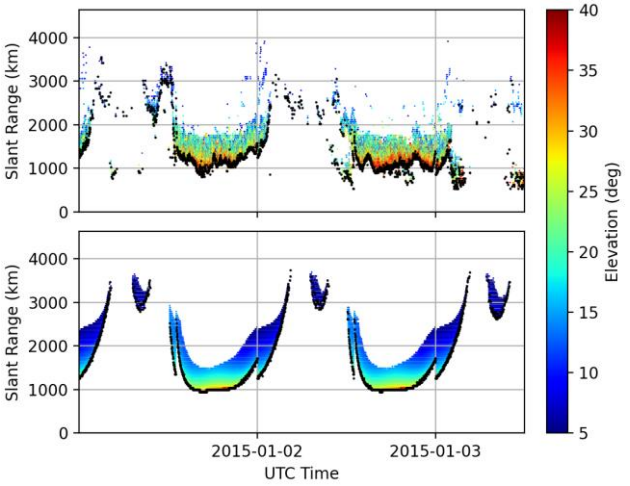

Figure 4. Time evolution of SuperDARN (A) and model (B) echo elevation angles after data processing.

To assess the variation in LE for both model and SuperDARN data, the time evolution of the LEs are plot along with the corresponding errors between the two data sets in Figure 5. Model and SuperDARN LEs generally show good agreement during the daytime, with errors in the order of approximately 50- to 300-km. Despite this, an increase in error is observed at 23:00 on the 3rd as the SuperDARN LE does not retreat in the same manner as for the previous day, which the simulation replicated moderately well. Errors become extremely significant as the daytime ionization disappears and reappears, as in these situations, minor time offsets, such as observed at 12:00 UT in both days, can manifest large LE errors due to the large LE gradients. The removal of ionization is predicted at a much slower rate by the model, as the gradient of the LE at approximately 00:00-03:00 UT is seen to be much lower than for SuperDARN on the 1st and 2nd. We can infer that the likely source of errors seen by the different LE gradients here is in the parameterization of hmF2 or NmF2, with either hmF2 increasing too rapidly in the evening or the opposite occurring for NmF2 at the same time. The impact of ionospheric scatter polluting the GB data is seen to be extremely significant at 03:00 on the 3rd

as highlighted previously, with these manifesting errors exceeding 1000 km, which would be catastrophic if not correctly identified in the context of a CR system. It is clear from Figure 5 that the use of GB LE for model assessment is extremely sensitive to differences in the ionospheric model and so provides a useful validation parameter.

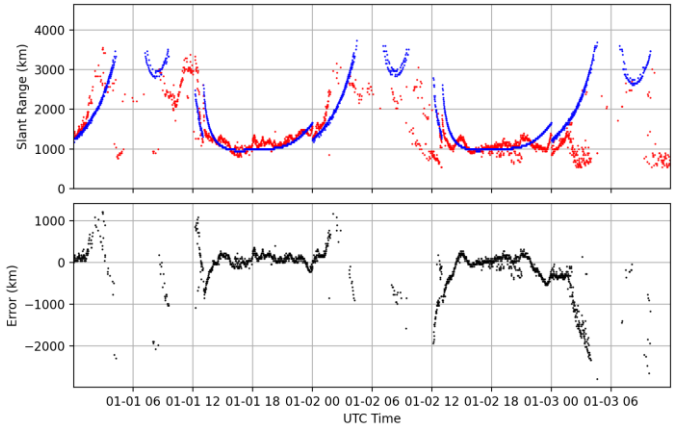

Figure 5. Time evolution of model and SuperDARN LE in blue and red, respectively. Relative errors are presented in the bottom panel.

The model represented the LE as expected, as the monthly median IRI model is simply not designed to capture the ionospheric variations at the temporal resolutions of interest here which clearly are the source of error if one focusses on the daytime LE. It is expected that the use of ionospheric models utilizing data assimilation schemes will show much reduced errors in LE due to their better representation of the immediate ionosphere, especially if SuperDARN GB data is potentially incorporated into the assimilation.

Conclusion

The validation of propagation models is essential to ensure applications employing HF raytracing can accurately reconstruct expected signal paths, with this being critical in the context of OTHR CR. This work has explored the use of SuperDARN GB for the validation and diagnosis of ionospheric models using 2D NRT, further increasing the utility of this expansive data set. The LE of model and SuperDARN echoes was successfully extracted and assessed, with errors in the order of 50km to 300km observed for the IRI2016 model during the daytime. Periods where echoes not associated with 1-hop F-mode contaminated the SuperDARN data were seen to introduce large errors when compared to model LE data. Errors in LE were seen to be significant during the morning and evening where the LE is seen to change considerably with time, highlighting the sensitivity of this method to diurnal variations within the ionosphere. Further work is required to develop this validation technique and to fully exploit this method for diagnosis of errors within ionospheric models.

Acknowledgements

The SuperDARN data used in this study was accessed through the University of Saskatchewan's SuperDARN data repository. The Blackstone SuperDARN radar is operated by the Virginia Tech Center for Space Science and Engineering Research. We are very grateful to these groups for their support of this work and their continuing provision and maintenance of this data.

References

[1] Thayaparan, T., Hum, R., Polak, J., Riddolls, R., *Ionospheric condition monitoring system for over-the-horizon radar (OTHR) in Canada*. in *2017 18th International Radar Symposium (IRS)*. 2017.

[2] Nishitani, N., et al., *Review of the accomplishments of mid-latitude Super Dual Auroral Radar Network (SuperDARN) HF radars.* Progress in Earth and Planetary Science, 2019. **6**(1): p. 27.

[3] Greenwald, R.A., Baker, K.B., Hutchins, A., Hanuise, C., *An HF phased-array radar for studying small-scale structure in the high-latitude ionosphere.* Radio Science, 1985. **20**(1): p. 63-79.

[4] Ponomarenko, P., Nishitani, N., Oinats, A.V., Tsuya, T., St-Maurice, J.P., *Application of ground scatter returns for calibration of HF interferometry data.* Earth, Planets and Space, 2015. **67**(1): p. 138.

[5] Bland, E.C., McDonald, A.J., Larquler, S.D., Devlin, J.C., *Determination of ionospheric parameters in real time using SuperDARN HF Radars.* Journal of Geophysical Research: Space Physics, 2014. **119**(7): p. 5830-5846.

[6] Ponomarenko, P.V., St-Maurice, J.P., Hussey, G.C., Koustov, A.V., *HF ground scatter from the polar cap: Ionospheric propagation and ground surface effects.* Journal of Geophysical Research: Space Physics, 2010. **115**(A10).

[7] Oinats, A.V., Nishitani, N., Ponomarenko, P., Ratovsky, K.G., *Diurnal and seasonal behavior of the Hokkaido East SuperDARN ground backscatter: simulation and observation.* Earth, Planets and Space, 2016. **68**(1): p. 18.

[8] Perry, G.W., Ruzic, K.D., Sterne, K., Howarth, A.D., Yau, A.W., *Modeling and Validating a SuperDARN Radar's Poynting Flux Profile.* Radio Science, 2022. **57**(3): p. e2021RS007323.

[9] Coleman, C. J. *A ray tracing formulation and its application to some problems in over-the-horizon radar*. Radio Science, 1998. **33**(4): 1187-1197.

[10] Sterne, K.T., Greenwald, R.A., Baker, J.B.H, Ruohoniemi, J.M. *Modeling of a twin terminated folded dipole antenna for the Super Dual Auroral Radar Network (SuperDARN)*. in *2011 IEEE RadarCon (RADAR)*. 2011.